Construction of a Statistical Atlas of the Whole Heart from a Large 4D CT Database

Karim Lekadir[1], Corné Hoogendoorn[1], Nicolas Duchateau[1], Alejandro F Frangi[1,2]

[1]Universitat Pompeu Fabra, Barcelona, Spain
[2]University of Sheffield, Sheffield, United Kingdom

Abstract

We present in this work an efficient and robust framework for the construction of a high-resolution and spatio-temporal atlas of the whole heart from a database of 138 CT 4D images, the largest sample to be used for cardiac statistical modeling to date. The data is drawn from a variety of pathologies, which benefits its generalization to new subjects and physiological studies. In the proposed technique, spatial and temporal normalization based on non-rigid image registration are used to synthesize a population mean image from all CT image. With the resulting transformation, a detailed 3D mesh representation of the atlas is warped to fit all images in each subject and phase. The obtained level of anatomical detail (a total of 13 cardiac structures) and the extendability of the atlas present an advantage over most existing cardiac models published previously.

1. Introduction

Statistical models play an increasingly important role in computational physiology of any organ, including the heart [1]. They provide not only an average layout of structures within an encapsulating structure, but also encode deviations from this average. This provides a means to deform the encapsulating structure, within statistically justified bounds, and have the substructures deform and move accordingly based on their statistical correlation. This enables two very important applications of computational physiology: first, simulation studies can be personalized geometrically. For geometrical personalization, the atlas can be matched to medical imaging data. Secondly, the statistics learned from the population can be used to generate populations for virtual population studies [2].

The construction of a statistical atlas from a population of images requires that each of the structures in the atlas be segmented (labeled) in each of the images in the database. To do this manually is generally considered an impossibility for 3D and 3D+time atlases. To bypass this problem, atlas-based segmentation methods provide a solution, particularly used for static organs such as the brain [3, 4]. First, one applies spatial normalization to the population. This is the synthesis of an average image from the population, usually based on image registration techniques. Additionally, it provides the spatial relationships between the population and this average. As one then labels this atlas, one may consider all the population images segmented through these spatial relationships. By representing the atlas as a surface mesh, one uses point distribution analysis as the approach to statistical analysis.

In practice, however, spatial normalization in the case of the heart is faced with a number of challenges, in particular the need to handle large and highly variable dynamic image datasets, the multi-region nature of the heart, and the presence of complex as well as small cardiovascular structures. In this work, we develop an efficient and robust framework for the construction of a high-resolution and spatio-temporal atlas of the whole heart that resolves the challenges listed above. The database of 138 CT 4D images used in this work is the largest sample to be used for cardiac statistical modeling to date. The data is drawn from a variety of pathologies, which benefits its generalization to new subjects and physiological studies. With the obtained statistical atlas, the level of detail (a total of 13 cardiac structures, see Table 1) and the extendability of the atlas present an advantage over most cardiac models published previously.

2. Methods

2.1. 4D image database

We firstly describe the database of imaging data used in this study, which was retrospectively collected from a cohort of 138 consecutive patients that underwent a CT examination as part of their routine diagnostic protocol for suspected coronary artery disease. All information was anonymized before its transfer from the clinic to our group. The patients were scanned using a Toshiba Aquilion 64 machine, with a Xenetix 350 contrast agent

of 80-100 ml at 5ml/s. The imaging resolution equals 0.4 x 0.4 x 2.0 mm, with an in-plane grid of 512 x 512 pixels, and an axial grid of 65.3 ± 11.3 slices. A total of 15 volumes were acquired per cardiac cycle for each subject.

While our database is not as large as that of the CAP [5], our image resolution is 2.5 to 5 times higher in-plane, and 3 to 4 times higher axially. This enables us to capture more anatomical detail than would be possible with clinical resolution MR data. Similarly, ultrasound has the advantages of non-invasiveness and higher temporal resolution, but these are undone by the speckle patterns which make automated further processing -specifically inter-subject registration- extremely difficult.

Table 1. Atlas subparts and element statistics

	Vertex count	Vertex density (cm^{-2})
1. LV myocardium	2032	10.66
2. Intraventricular septum	1492	12.40
3. RV myocardium	3454	10.70
4. LA myocardium	2010	11.68
5. RA myocardium	1962	10.90
6. Aorta	2654	9.40
7. Vena cava	742	11.25
8. Pulmonary trunk/artery	1032	11.46
9. Pulmonary veins	1232	10.27
10. Ant. descending artery		
11. Circumflex artery		
12. Diagonal artery		
13. Right coronary artery		

2.2. Reference selection

We now describe the main steps involved in the proposed framework. The idea behind the proposed technique is to manually segment a reference image volume, which is then non-rigidly registered to the entire set of image volumes for all subjects and time frames. The manual 3D reference shape is subsequently propagated to all image volumes based on the registration transformations, thus obtaining a full set of segmented 4D image data, from which a statistical atlas and statistical shape model can be derived.

In the proposed framework, the selection of a suitable reference is a critical step in order to minimize bias in the synthesized mean volume. This is particularly important in the case of a large 4D database such as the one used in this study as it involves significant spatial and temporal variability (we have a total of 2010 image volumes). Choosing an appropriate reference image also reduces the time complexity that is an issue for such demanding tasks. Therefore, the first step of the proposed workflow is an attempt to select the reference as close as possible to the unknown mean. For this we use a heuristic based on a Groupwise Mutual Information (GWMI) score, an extension of Mutual Information [6] that describes the amount of information between a single image $\mathbf{I}$ and a set of images Γ [7], i.e.,

$$\mathrm{GWMI}(\mathbf{I},\Gamma) = H(\mathbf{I}) + H(\Gamma) - H(\mathbf{I},\Gamma)$$

where H denotes the Shannon entropy. We compute the GWMI score over affinely registered volumes. The score represents the amount of information each volume carries with respect to the remainder of the volumes, taking into account the variation observed in this set. To make the process even more robust to the reference volume used in the affine registration, we registered all images affinely to 11 randomly selected volumes, and applied GWMI to each of the 11 resulting sets of 138 volumes, obtaining 11 rankings. The reference ultimately chosen for the atlas construction is the volume with the best mean rank.

2.3. Diffeomorphic registration

With the reference subject chosen from the population as described in the previous section, we register the volume corresponding to each subject's first cardiac phase to the first phase of the reference subject. The first step of this registration is a global affine registration, requiring few parameters to optimize. It has been shown that such an approach increases the robustness of the overall scheme [8].

Following the affine registration, nonrigid registration is used to resolve the remaining variations between the reference and population images. With a large number of registrations to be carried out, a fast registration approach is desirable. The multiscale approach using B-splines fulfils this criterion. In the original formulation of the diffeomorphic B-splines, new splines were added until convergence of the registration. However, we choose to maintain a fixed set of transforms. This results in control over the maximum possible local deformation, and therefore prevents the construction of outliers that could corrupt the computation of the mean deformation.

Using T for transformations obtained by composition of transforms, A^s for the affine transformation from the reference subject to subject s, B^s for a B-spline based deformation from the reference subject to subject s, $B^{s,\tau}$ for the B-spline based deformation for the nonrigid deformation from frame $\tau-1$ to frame τ of subject s, the total transformation to frame τ of subject s is given by:

$$T^{s,\tau}_{\text{total}} = T^{s,\tau}_{\text{intra}} \circ T^{s}_{\text{inter}} \circ A^s$$

$$\text{where } T^{s,\tau}_{\text{intra}} = \square_{t=2}^{\tau} B^{s,t} \text{ and } T^{s}_{\text{inter}} = \square_{i=1}^{n_b} B^{s}_{i}$$

Here, n_b is the number of B-spline transforms we use to

compose the deformation from the reference to subject s, and $\square$ is the big version of the composition operator $\circ$. After the affine registration has brought the images into a global alignment, by controlling the spline control point spacing and n_b we control the maximum total local deformation.

After the non-rigid registration, we represent the inter-subject transformations T^s_{inter} as displacement vector fields, thus simplifying further processing in the absence of the composition operators. The use of B-splines to model our deformation reduces the number of degrees of freedom in the optimization problems by multiple orders of magnitude as compared to a parameter-free approach that directly produces a vector field, like the diffeomorphic demons [9].

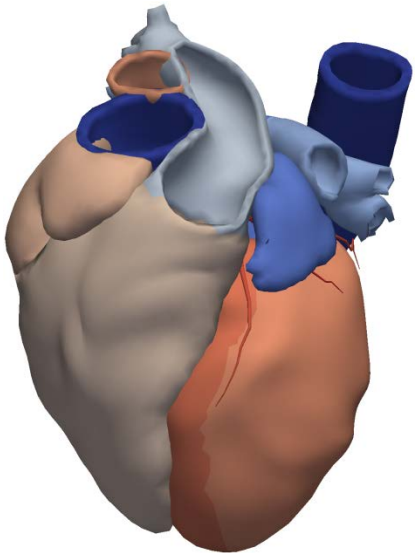

Fig. 1. The full atlas mesh corresponding to the synthetized mean image. Different colors indicate different structures.

3. Experiments and results

The quality of the obtained cardiac models depends on the quality of the registration, which is firstly evaluated in this validation. To this end, random selection of volumes and slices is achieved since the dataset size does not enable to fully delineate volumes for all the selected subjects. We then calculate the registration accuracy by using distance-based measures between the gold standard and the automatic result (Table 2), as well as an overlap F-metric (Table 3).

The results reported in Table 2 provide insight into the agreement on key cardiac boundaries and anatomical landmarks. The average distance of the contours ranges from 1.59 mm for the left ventricular area to 2.76 mm for the right atrial area. This compares favorably with the slice spacing of 2.0 mm. The difference in performance between the left ventricular area and the atrial and right ventricular areas is easily explained by the low complexity of the LV compared to the atria, and the much smaller influence of trabeculation on the LV blood-myocardium boundary strength. The landmark errors also compare well with the interobserver variation for the valves and the left coronary origin. The greater error in the apex is due to a sliding along the LV cavity wall; it is on the boundary but not at the apical point. During registration, boundaries are matched yet boundary curvature, by which observers would identify the apex, is not taken into account. The difference between interobserver variation and registration error of the right coronary artery (RCA) origin is due to the size of the RCA. While its position is stable at the base of the aorta, its appearance is often weak, thus offering no boundary for the registration to match.

Table 2. Registration error (mm) for all structures.

	Interobserver error (mm)	Registration error (mm)
1. Aorta		2.19 ± 1.81
2. LV cavity		1.83 ± 0.64
3. LV myocardium		1.59 ± 0.45
4. RV cavity		2.45 ± 0.87
5. LA cavity		2.31 ± 1.73
6. RA cavity		2.76 ± 1.21
1. LV endo. apex	5.03 ± 2.97	9.28 ± 10.12
2. Aortic valve center	4.40 ± 2.88	5.40 ± 8.47
3. Mitral valve center	7.31 ± 3.87	9.82 ± 12.04
4. Left coron. origin	3.76 ± 2.18	5.50 ± 6.86
5. Right coron. origin	2.52 ± 2.54	9.22 ± 7.88

Table 3. Registration overlap (F-score).

	F-score
1. Aorta	0.85 ± 0.15
2. LV cavity	0.92 ± 0.02
3. LV myocardium	0.77 ± 0.05
4. RV cavity	0.82 ± 0.07
5. LA cavity	0.72 ± 0.13
6. RA cavity	0.64 ± 0.16
7. Left blood	0.90 ± 0.05
8. Right blood	0.82 ± 0.07

The overlap-based accuracy is reported in Table 3 as F-scores in the atlas space, where we listed both the mean and standard deviations per structure. It shows overall a good overlap between the manual contours and those obtained with the implemented registration.

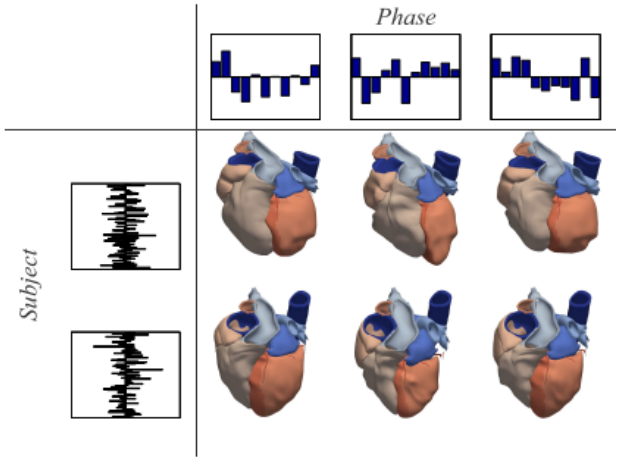

Fig. 2. Three phases of two subjects, with their bilinear parameter sets derived from the full subject data set. The dimensionality of the phase and subject parameters (11 and 115, respectively) are based on explaining 95% of total variance for each axis.

Following the application of the proposed workflow, a training set of multi-structure 4D cardiac meshes is available for furthermore processing. From these, a full atlas mesh corresponding to the synthesized mean image is obtained, as displayed in Fig. 1. The structures outlined are colored separately in the figure. For the left ventricle, the myocardium and blood pool were segmented, while for both atria, for the right ventricle and for the trunk of the aorta, the blood pool was segmented.

Furthermore, we applied a statistical decomposition using bilinear models [10] which enables to decouple the variation due to the subject-specific morphology and to the cardiac motion. Fig. 2 shows three phases of four subjects, together with bar plots for their subject and phase parameters. The atlas and statistical models are made available for public downloading: http://www.cistib.upf.edu/cistib/index.php/download.

4. Discussion and conclusions

We presented an efficient and robust workflow to construct detailed spatiotemporal models of the heart. Its flexibility means the obtained statistical atlas can be used for various model-based image analysis tasks, as well as in cardiac simulation, which is the subject of our future work.

Acknowledgements

This work was partly funded by the euHEART project from the FP7 of the European Union, partly by a CDTI CENIT-cvREMOD grant of the Spanish Ministry of Science and Innovation, and partly by the Spanish Ministry Science and Innovation (STIMATH project - ref. TIN2009-14536-C02-01).

References

[1] Camara O, Konukoglu E, Pop M, Rhode K, Sermesant M, Young AA. Proceedings of the second international workshop on statistical atlases and computational models of the heart (STACOM): Imaging and modelling challenges. Lecture Notes in Computer Science, 2012. 7085.

[2] Young AA, Frangi AF. Computational cardiac atlases: From patient to population and back. Experimental Physiology 2009;94(5): 578–596.

[3] Rueckert D, Frangi AF, Schnabel JA. Automatic construction of 3D statistical deformation models of the brain using non-rigid registration. IEEE Transactions on Medical Imaging, 2003;22(8):1014-1025.

[4] Jongen C, Pluim JPW, Nederkoorn PJ, Viergever MA, Niessen WJ. Construction and evaluation of an average CT brain image for inter-subject registration. Computers in Biology and Medicine 2004;34(8): 647–662.

[5] Fonseca CG, Backhaus M, Bluemke DA, Britten RD, Chung JD, Cowan BR, Dinov ID, Finn JP, Hunter PJ, et al. The cardiac atlas project–an imaging database for computational modeling and statistical atlases of the heart. Bioinformatics 2011; 27(16): 2288–2295.

[6] Maes F, Collignon A, Vandermeulen D, Marchal G, Suetens P. Multimodality image registration by maximization of mutual information. IEEE Transactions on Medical Imaging 1997;16(2):187–198.

[7] Hoogendoorn C, Whitmarsh T, Duchateau N, Sukno FM, Craene MD, Frangi AF. A groupwise mutual information metric for cost efficient selection of a suitable reference in cardiac computational atlas construction. in Proc. of SPIE Medical Imaging 2010.

[8] Rueckert D, Sonoda LI, Hayes C, Hill DLG, Leach MO, Hawkes DJ. Nonrigid registration using free-form deformations: Application to breast MR images. IEEE Transactions on Medical Imaging 1999; 18(8):712-721.

[9] Vercauteren T, Penne CX, Perchant A, Ayache N. Diffeomorphic demons: Efficient non-parametric image registration. NeuroImage 2009; 45(1): S61-S72.

[10] Hoogendoorn C, Sukno FM, Ordas S, Frangi AF. Bilinear models for spatio-temporal point distribution analysis: Application to extrapolation of left ventricular, biventricular and whole heart cardiac dynamics. International Journal of Computer Vision 2009; 85(3): 237–252.

Address for correspondence.

Karim Lekadir
Universitat Pompeu Fabra
Department of Information & Communication Technologies
08018 Barcelona, Spain

E-mail: karim.lekadir@upf.edu